

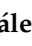
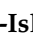




Article

Kinetics of Thermal Decomposition of Carbon Nanotubes Decorated with Magnetite Nanoparticles

Rubén H. Olcay¹, Elia G. Palacios² , Iván A. Reyes^{3,4} , Laura García-Hernández⁵, Pedro A. Ramírez-Ortega⁵, Sayra Ordoñez⁵, Julio C. Juárez⁶ , Martín Reyes⁶ , Juan-Carlos González-Islas⁷  and Mizraim U. Flores^{2,5,*} 

- ¹ Departamento de Metalurgia y Minas, Facultad de Ingeniería y Arquitectura, Universidad Arturo Prat, Iquique 1110939, Chile
- ² Escuela Superior de Ingeniería Química e Industrias Extractivas-IPN, Unidad Profesional Adolfo López Mateos, Zacatenco 07738, Mexico
- ³ Instituto de Metalurgia, Universidad Autónoma de San Luis Potosí, San Luis Potosí 78210, Mexico; alejandro.reyes@uaslp.mx
- ⁴ Consejo Nacional de Humanidades Ciencias y Tecnologías, Benito Juárez 03940, Mexico
- ⁵ Área Electromecánica Industrial, Universidad Tecnológica de Tulancingo, Camino a Ahuehuetitla, #301 Col. Las Presas, Tulancingo 43642, Mexico
- ⁶ Área Académica de Ciencias de La Tierra y Materiales, Universidad Autónoma del Estado de Hidalgo, Carretera Pachuca-Tulancingo km 4.5, Carboneras 42184, Mexico
- ⁷ Instituto de Ciencias Básicas e Ingeniería, Universidad Autónoma del Estado de Hidalgo, Carretera Pachuca-Tulancingo km 4.5, Carboneras 42184, Mexico
- * Correspondence: mflores@utectulancingo.edu.mx

Abstract: Magnetite nanoparticles were synthesized using the green chemistry technique; ferric chloride was used as a precursor agent and *Moringa oleifera* extract was used as a stabilizer agent. A black powder, characteristic of magnetite, was obtained. X-ray diffraction was performed on the synthesis product and identified as magnetite (Fe₃O₄). Scanning electron microscopy characterization shows that nanoparticles have a spherical morphology, with sizes ranging from 15 nm to 35 nm. The synthesis of carbon nanotubes was carried out by the pyrolytic chemical deposition technique, from which multiwalled carbon nanotubes were obtained with diameters of 15–35 nm and of varied length. The decoration was carried out using the wet and sonification technique, where a non-homogeneous coating was obtained around the nanotubes. The thermal decomposition for both decorated and undecorated nanotubes presents two mass losses but with different slopes, where the activation energy for the decorated carbon nanotubes was 79.54 kJ/mol, which shows that the decoration gives more stability to the nanotubes since the activation energy of the undecorated nanotubes is 25.74 kJ/mol.

Keywords: thermal stability; decorated carbon nanotubes; magnetite nanoparticles; kinetics analysis



Citation: Olcay, R.H.; Palacios, E.G.; Reyes, I.A.; García-Hernández, L.; Ramírez-Ortega, P.A.; Ordoñez, S.; Juárez, J.C.; Reyes, M.; González-Islas, J.-C.; Flores, M.U. Kinetics of Thermal Decomposition of Carbon Nanotubes Decorated with Magnetite Nanoparticles. *C* **2024**, *10*, 96. <https://doi.org/10.3390/c10040096>

Academic Editors: Jandro L. Abot and Giuseppe Cirillo

Received: 24 September 2024

Revised: 31 October 2024

Accepted: 13 November 2024

Published: 15 November 2024



Copyright: © 2024 by the authors. Licensee MDPI, Basel, Switzerland. This article is an open access article distributed under the terms and conditions of the Creative Commons Attribution (CC BY) license (<https://creativecommons.org/licenses/by/4.0/>).

1. Introduction

Carbon nanotubes are allotropes of carbon, such as diamond, graphene, or fullerenes; these nanotubes are formed by hexagonal arrangements of carbon that originate small cylinders that usually have a diameter within the range of the Armstrongs to a few tens of nm [1,2]. Carbon nanotubes (single or multiwalled) have become one of the most valuable one-dimensional (1D) nanomaterials due to their superior electrical, physical, and mechanical characteristics. Multiwalled carbon nanotubes (MW-CNTs) possess unique electrical properties resulting from the conjugated electron system between their carbon atoms and nearly 1D shape [3,4]. Carbon nanotubes have many applications due to the diversity of properties they present; however, applications in electronics, coatings, and batteries in fuel cells, super capacitors, sensors, and energy storage devices require that these nanotubes withstand high temperatures due to the overheating that these applications can present [3]. Recently, researchers have been increasingly interested in doped and decorated carbon nanotubes as they present better properties and a wide variety of applications due to

the unique properties they acquire [5–9]. Metal and non-metal doping are used for carbon nanotubes to regulate their thermal, physics, and electronic characteristics. For instance, substitutional doping is promising because dopants regulate the mechanical and electronic characteristics, leading to better response time, better sensitivity, a more compact size, and a low operating temperature, as studied for several use cases like biosensors, mechanical test, bactericidal agents [5,6], electronic instruments, and drug delivery [9–12]. Different techniques have been implemented to decorate carbon nanotubes; however, none have managed to achieve complete decoration, as there is always an uncovered surface. However, using a chemical method to deposit metals onto the oxidized nanotube surface results in a rather even distribution of the metals on the surface, but the density of decoration is low in many cases [13]. Even when elements/compounds with low surface tensions are melted onto the nanotube surface, the wetting of the surface is incomplete. The tube surface in all these cases does not catalyze the deposition of the metal/metal compound. This results in random deposition throughout the solution, not only on the surface of tubes. Nowadays, carbon nanotubes are being used in various areas where they are subjected to high temperatures. Numerous studies have shown that carbon nanotubes can either act as combustion catalysts alone or be applied as composites with metal compounds in composite solid propellants [14]. For examples, a number of carbon nanotube-encapsulated ferrocenes and transition metal compounds were fabricated recently by ultrasonic treatment, and these nanocomposites exhibited excellent combustion catalytic properties for organic compounds (AP, RDX, FX300, etc.), such as thermal decomposition [15–20]. The applications of carbon nanotubes at high temperatures are increasing every day (batteries in fuel cells, super capacitors, sensors and energy storage devices, among other applications), so it is important to understand their behavior and stability. In addition, it is important to improve their thermal properties and increase their stability at high temperatures. Due to the limited information on the thermal stability of carbon nanotubes decorated with metallic particles, in the present work, the synthesis of carbon nanotubes and magnetite nanoparticles was carried out, the decoration was carried out, and, in addition, a kinetic analysis of the thermal decomposition of said carbon nanotubes was performed before and after decoration.

2. Experimental Methodology

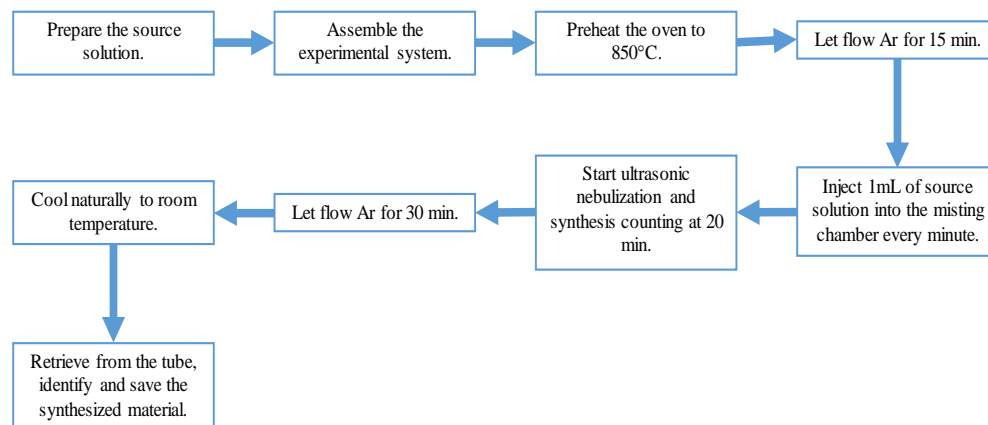
2.1. Synthesis of Magnetite Nanoparticles Using *Moringa Oleifera* Extract

The *Moringa oleifera* extract was obtained following the methodology of Altaf et al., 2021, from which 20 g of healthy leaves was weighed, washed with plenty of deionized water, dried at room temperature in a desiccator, and, once dry, they were added to a reactor at 85 °C for 20 min. Then, they were allowed to cool, filtered to remove excess solids, and finally centrifuged at 2000 rpm for 10 min to obtain a completely clean solution. *Moringa oleifera* extract was used as a reducing agent of ferrous chloride to Fe₃O₄ nanoparticles since it is an economical and environmentally friendly method, and particles smaller than 50 nm were obtained. Four syntheses of magnetite nanoparticles were carried out using the extract of *Moringa oleifera*. In addition, 0.1 M of ferric chloride and 0.05 M of ferrous chloride were used as precursors, and both were of reagent grade. A total of 1 M of sodium hydroxide was used as a pH stabilizer in 100 mL of the extract. Each of the syntheses was under constant magnetic stirring of 1200 rpm; the synthesis temperature was 55 °C. At the end of each experiment, a black powder was recovered, which was the magnetite nanoparticles [21].

2.2. Synthesis of Carbon Nanotubes

For the synthesis of nanotubes, a source solution was prepared with the following percentages: 5% ferrocene, 2.5% ethanol, and 92.5% toluene [22]. The synthesis conditions were 20 mL of source solution, temperature of 850 °C, 1380 mL/min of argon, and 20 min of synthesis. The synthesis procedure was as follows: The oven was heated to the synthesis temperature, Ar was allowed to flow for 15 min, 1 mL of source solution was injected into the nebulization chamber every minute, ultrasonic nebulization was started, and the

synthesis time was counted. Once the synthesis was complete, Ar was allowed to flow for 30 min and then the temperature of the furnace was lowered with natural cooling to room temperature. The synthesized material was recovered from the tube, identified, and stored. Scheme 1 summarizes the synthesis of carbon nanotubes.



Scheme 1. Methodology for the synthesis of carbon nanotubes.

2.3. Decoration of Carbon Nanotubes

For the decoration of the carbon nanotubes with the magnetite nanoparticles, the technique reported by Hamouda et al. (2021) [23] was carried out, which is known as wet decorated, which consists of placing the carbon nanotubes in an ethanol solution under ultrasound for 30 min, and during this time, the magnetite nanoparticles are added drop by drop until there is an impregnation on the surface of the nanotubes [23]. The solution is then centrifuged at 4000 rpm for 5 min and the solids are recovered, which will be the carbon nanotubes decorated with magnetite nanoparticles.

2.4. Characterization

To verify the presence of carbon nanotubes and magnetite nanoparticles, X-ray diffraction was performed (Bruker D8 powder diffractometer, Billerica, MA, USA with Ni-filtered radiation from a Cu anode, $k_{\alpha 1} = 1.5406 \text{ \AA}$; 40 kV and 35 mA). Diffraction patterns were recorded in the angular range 2θ of $10\text{--}90^\circ$ with a step size = 0.01° and a step time = 3 s. For thermal characterization, thermogravimetric analysis was carried out on a Mettler-Toledo TGA/DTA 851e (Greifensee, Switzerland). The experiments were performed with a heating of 10 K min^{-1} using air with a flow of $666 \times 10^{-3} \text{ m}^3 \text{ s}^{-1}$.

2.5. Methodology to the Thermal Decomposition Kinetics

The kinetic analysis was carried out isothermally using the method known as “time to a given fraction”. The mass fractions of each of the temperatures used in each mass loss ramp were determined. For each of the stages, 4 temperatures that form part of the mass loss slope were taken, and the kinetic method known as “time to given fraction” was then applied to determine the activation energy of each of the mass losses, applying the Arrhenius equation [24–28].

3. Results and Discussion

3.1. Characterization of Carbon Nanotubes and Magnetite Nanoparticles

By means of X-ray diffraction (Figure 1), the characteristic crystallographic planes of carbon nanotubes have been identified; these planes are shown at 26° and 44° . The most intense crystallographic plane is 002; the crystallographic plane is 100, which is less intense, but it is also characteristic of carbon nanotubes.

The X-ray diffraction spectrum of magnetite nanoparticles is shown in Figure 2, where the most intense characteristic crystallographic planes are the (311), (200), (400), (511), and

(440) planes. These crystallographic planes correspond to the crystallographic chart ICDD-PDF 01-071-6336, which belongs to magnetite, which has been used to decorate carbon nanotubes. Magnetite has a face-centered cubic crystal structure with a lattice parameter of 8.3578 Å and a density of 5.27 g/cm³.

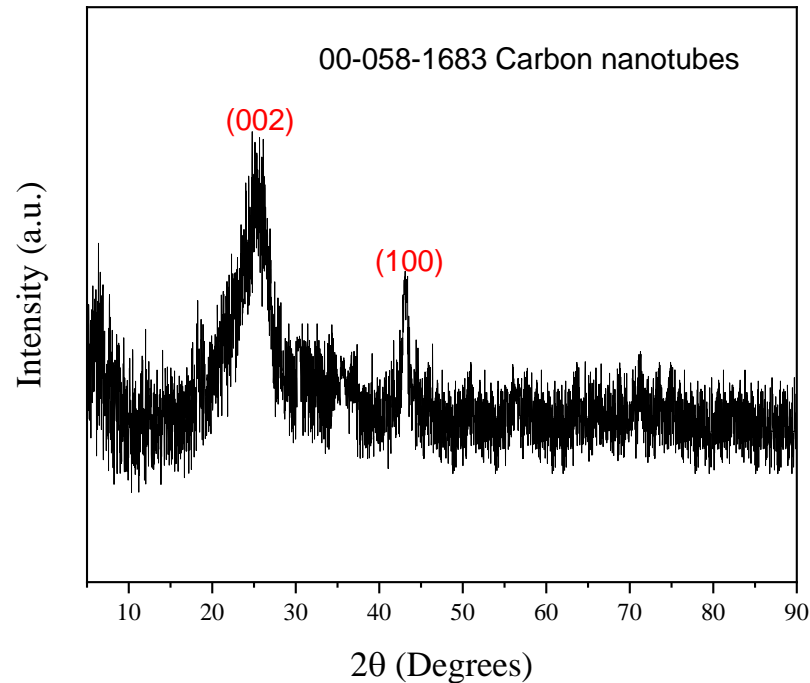


Figure 1. X-ray diffraction spectrum of carbon nanotubes.

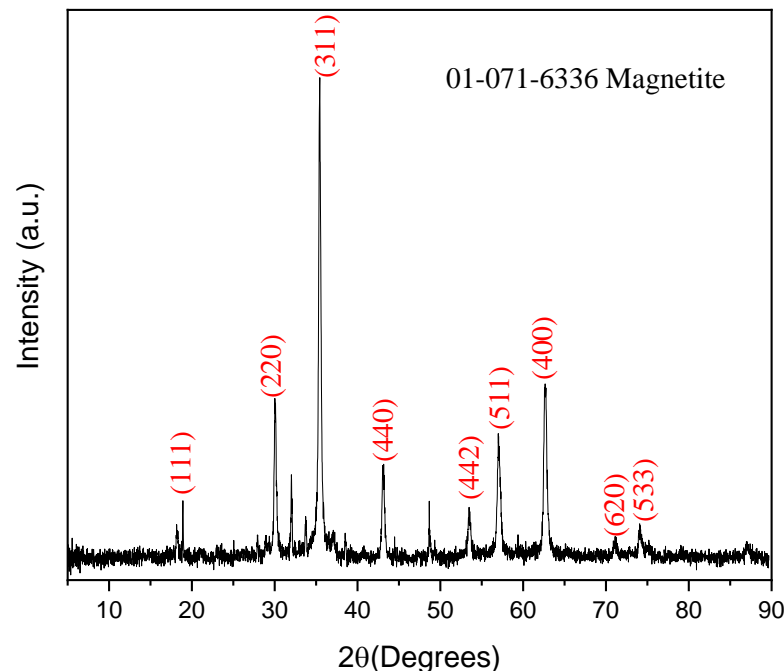


Figure 2. X-ray diffraction spectrum of magnetite particles.

Using scanning electron microscopy, the morphology and size of the magnetite nanoparticles were determined (Figure 3a). It was observed that they have sizes ranging from 15–35 nm, which will favor the decoration of the nanotubes since they are similar in size to the diameters observed in said nanotubes (Figure 3b). The decoration of the nanotubes occurs superficially. Figure 3c shows how the magnetite nanoparticles surround

the carbon nanotubes, creating a shell that will allow the nanotubes to withstand higher decomposition temperatures. The proportion used for the decoration was 1:3 magnetite nanoparticles/carbon nanotubes. Figure 3d shows decorated nanotubes at 100,000X.

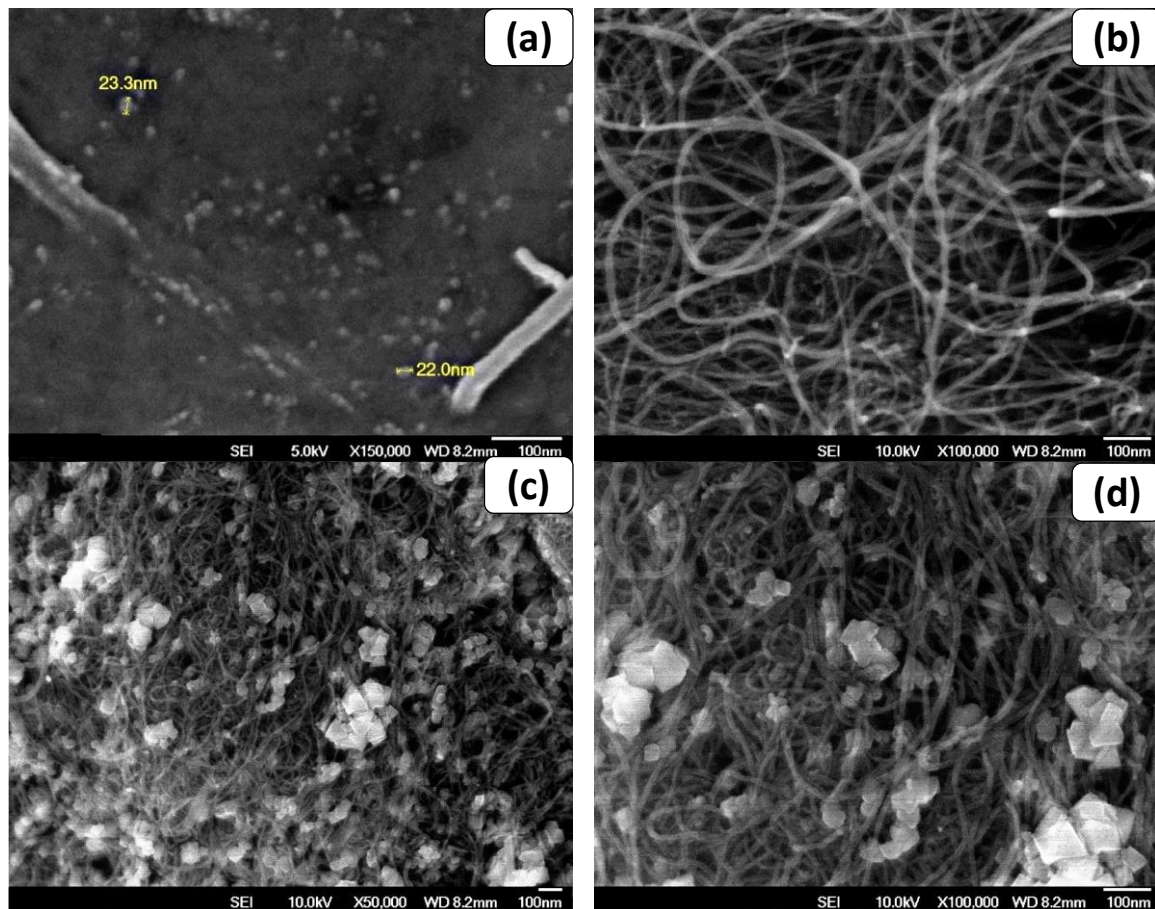


Figure 3. SEM images of (a) the nanoparticles with diameters of 30 nanoparticles with diameters of 30 nm; (b) carbon nanotubes with diameters of 25 nm; (c) carbon nanotubes decorated with the magnetite nanoparticles viewed at 50,000X; (d) carbon nanotubes decorated with the magnetite nanoparticles viewed at 100,000X.

To confirm that the carbon nanotubes are decorated with magnetite nanoparticles, X-ray diffraction was performed, which confirmed that both phases are present, as shown in Figure 4. The characteristic crystallographic planes of both species appear in the diffraction spectrum, with those of magnetite being more intense due to their high crystallinity. On the other hand, the less intense planes belong to the carbon nanotubes, thus confirming the decoration.

The differential thermal analysis and its derivative of the carbon nanotubes, observed in Figure 5a, shows that there are two mass losses: the first loss begins at 80 °C and ends at 185 °C with a maximum conversion at 90 °C which can be attributed to the presence of water that has adsorbed the sample; this is due to the high hygroscopicity of the carbon nanotubes. The first mass loss is 9.2%, so in addition to water, the reagents used during the synthesis could have decomposed. The second mass loss begins at 185 °C and ends at 800 °C, which is where the experiment ended, so this loss is attributed to the decomposition of the carbon nanotubes. The maximum conversion of this decomposition occurred at 280 °C. Figure 5b shows the thermogravimetric analysis and its derivative of the magnetite nanoparticles. This thermogram does not show mass losses since it is a stable oxide and does not present any stage from room temperature to 800 °C. However, curves are shown at 200 °C and 600 °C, which are considered noise because the mass loss in these stages is less than 1%. The thermal behavior of the magnetite nanoparticles will be the same

throughout the decomposition of the carbon nanotubes since these nanoparticles do not show a variation in mass as the temperature increases.

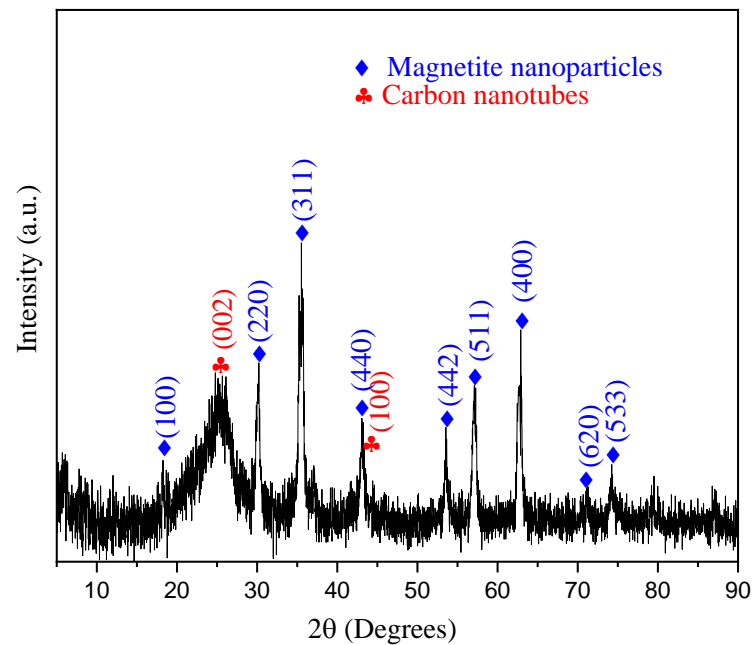


Figure 4. X-ray diffraction spectrum of carbon nanotubes decorated with magnetite nanoparticles.

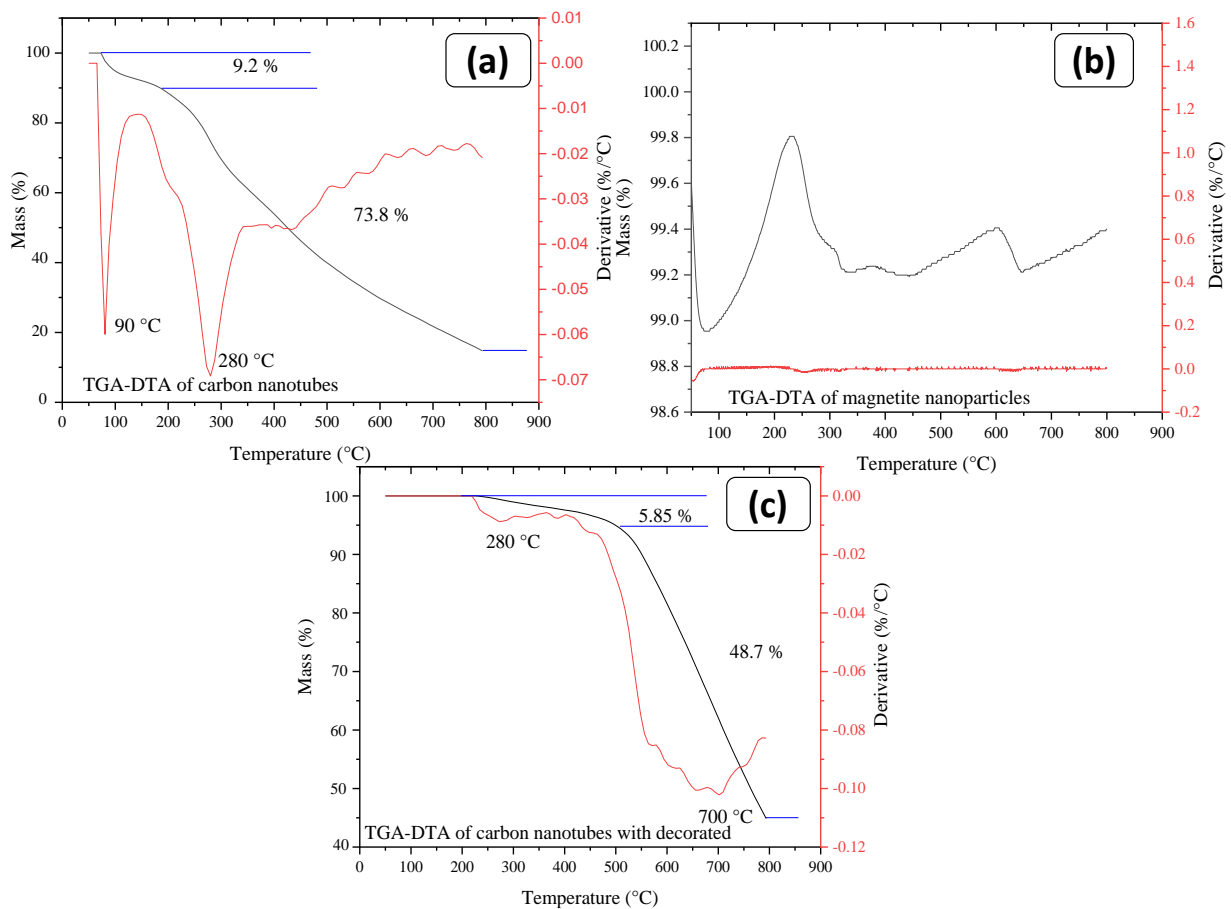


Figure 5. (a) Differential thermogravimetric analysis of carbon nanotubes; (b) differential thermogravimetric analysis of magnetite nanoparticles; (c) differential thermogravimetric analysis of carbon nanotubes decorated with magnetite nanoparticles.

Figure 5c shows the differential thermal analysis and its derivative of the carbon nanotubes decorated with magnetite nanoparticles. Here, two mass losses are also observed: The first loss begins at 230 °C and ends at 500 °C and is attributed to the carbon nanotubes that are not decorated, which are approximately 5.85%, indicating that a small percentage of nanotubes have remained undecorated. The second mass loss is 48.7% and is attributed to the decomposition of the decorated carbon nanotubes. Here, it is observed that the slope begins at 500 °C and ends at the temperature programmed for the analysis, so the temperature range is lower than in the second loss in Figure 5a, so it is expected that there will be a higher activation energy for this stage.

3.2. Thermal Decomposition Kinetics

To determine the activation energy of the thermal decomposition of the carbon nanotubes and carbon nanotubes decorated with magnetite nanoparticles, the mass fraction of the decomposition reaction was calculated with Equation (1):

$$y = \frac{m_0 - m_t}{m_0 - m_f} \quad (1)$$

where y is the mass fraction that has reacted, m_0 is the initial mass, m_t is the mass at a given time, and m_f is the final mass that has remained after the experiment has ended [24–26].

Once the mass fraction is obtained, the kinetic model called “time to given fraction” is applied; with this model, the experimental rate constant is obtained at different temperatures (four temperatures for each mass loss) for a time (t), whose transformed fraction has been taken as $y = 0.5$, with which the activation energy is calculated according to Equation (2).

$$\frac{dy}{dt} = k \cdot f(y) \quad (2)$$

The time t_y to transform a given fraction $y = Y$ is then

$$t_y = k^{-1} \int_{y=0}^{y=Y} f^{-1}(y) dy \quad (3)$$

where t_y is time at a given transformation stage, k is the experimental constant of rate, y is the transformed material fraction, and $f(y)$ is a function of y .

If the function, $f(y)$ does not change over the temperature range studied and the integral above has a constant numerical value, and therefore

$$t_y = k^{-1} \quad (4)$$

$$t_y = A^{-1} \exp\left(\frac{-E_a}{RT}\right) \quad (5)$$

Therefore,

$$\ln t_y = \ln A + \frac{E_a}{R} \left(\frac{1}{T}\right) \quad (6)$$

To determine the value of activation energy, $\ln t_y$ vs. $1/T$ is plotted, and the resulting slope is the value of E_a/R , and the ordered to the origin is the value of the Arrhenius constant or the number of coalitions between molecules before the reaction begins [24–26].

In order to carry out the thermal decomposition kinetics, thermogravimetric analysis (TGA) and differential thermal analysis were performed on the undecorated and decorated nanotubes. Figure 6a shows the isotherms of the first mass loss of the undecorated carbon nanotubes, where the activation energy is 6.75 kJ/mol (Figure 6b), which indicates that there is diffusive control since the water in the nanotubes is only desorbed on the surface and is not structural water, so little energy is required for it to evaporate. Figure 6c shows the isotherms of the second mass loss, which is attributed to the decomposition of the

carbon nanotubes, which begins at 185 °C and ends at 800 °C. The decomposition loss of carbon nanotubes presents a long slope (long temperature range), with a constant mass loss; this means that the increase in temperature is directly proportional to the mass loss. The temperatures used to calculate the activation energy of the second loss were 300, 400, 500, and 700 °C; the isotherms at these temperatures were also 10 min. The activation energy for the decomposition of undecorated carbon nanotubes (Figure 6d) is 25.74 kJ/mol, which indicates that there is both chemical and diffusive control and that both the increase in temperature and the diffusion of matter are those that control the decomposition reaction of this second mass loss.

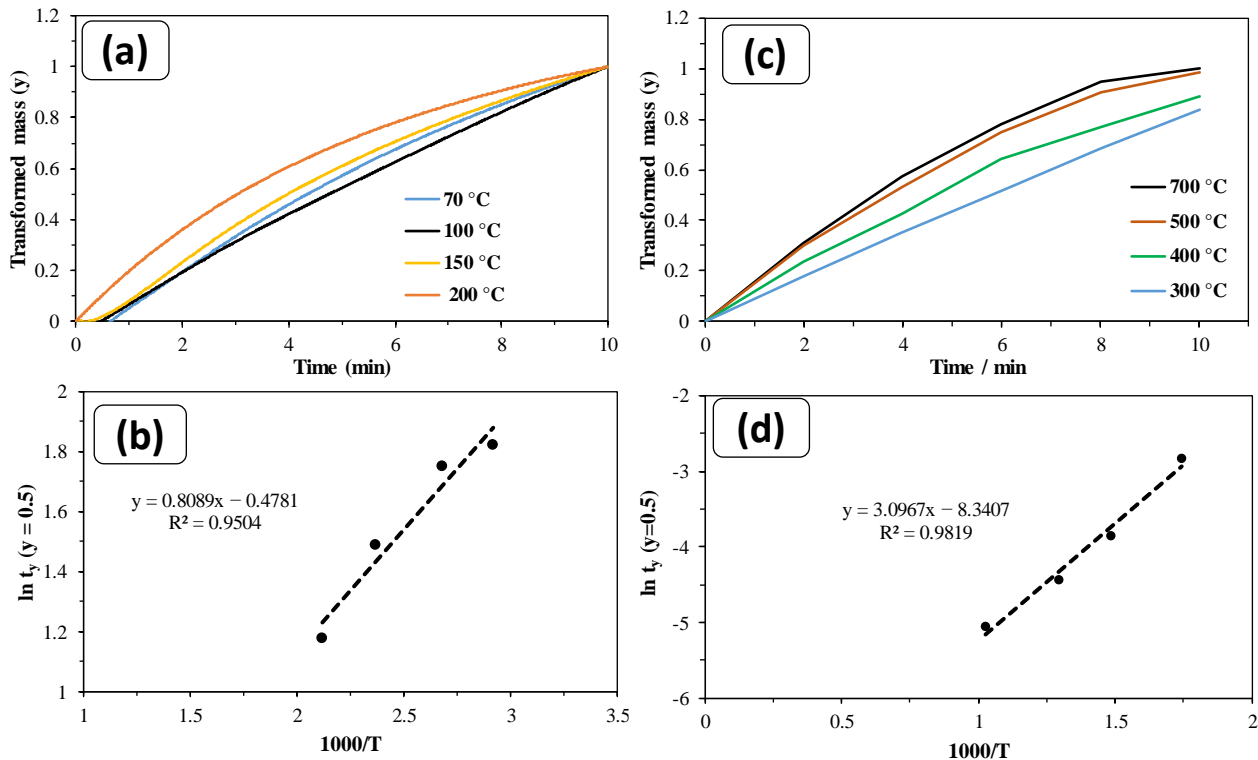


Figure 6. Kinetic analysis of thermal decomposition of carbon nanotubes. (a) First-stage mass loss isotherms; (b) calculation of the first-stage activation energy; (c) second-stage mass loss isotherms; (d) calculation of the second-stage activation energy.

The thermal decomposition of carbon nanotubes decorated with magnetite nanoparticles also presents two mass losses, but the behavior changes compared to undecorated carbon nanotubes since in this decomposition process, there is no long slope (short temperature range), so it is of a higher value compared to Figure 5a; in addition, there is no proportionality of the mass loss with respect to temperature since it is a thermally more stable compound. To determine the activation energy of the first loss, isotherms of 200, 300, 370, and 450 °C were used (Figure 7a), giving an activation energy value of 20.61 kJ/mol (Figure 7b), which indicates that both the temperature and the diffusion of matter are those that control the decomposition process of the first mass loss. For the second mass loss, isotherms of 520, 600, 700, and 800 °C have been used (Figure 7c), and the activation energy obtained is 79.54 kJ/mol (Figure 7d), which indicates that there is a temperature-controlled decomposition process, which makes the compound more stable, since three times more energy is required to decompose it compared to undecorated nanotubes. The transformed mass of carbon nanotubes decorated with magnetite nanoparticles increases as the temperature rises because the temperature range where the largest mass loss takes place is very short compared to the temperature range of undecorated carbon nanotubes.

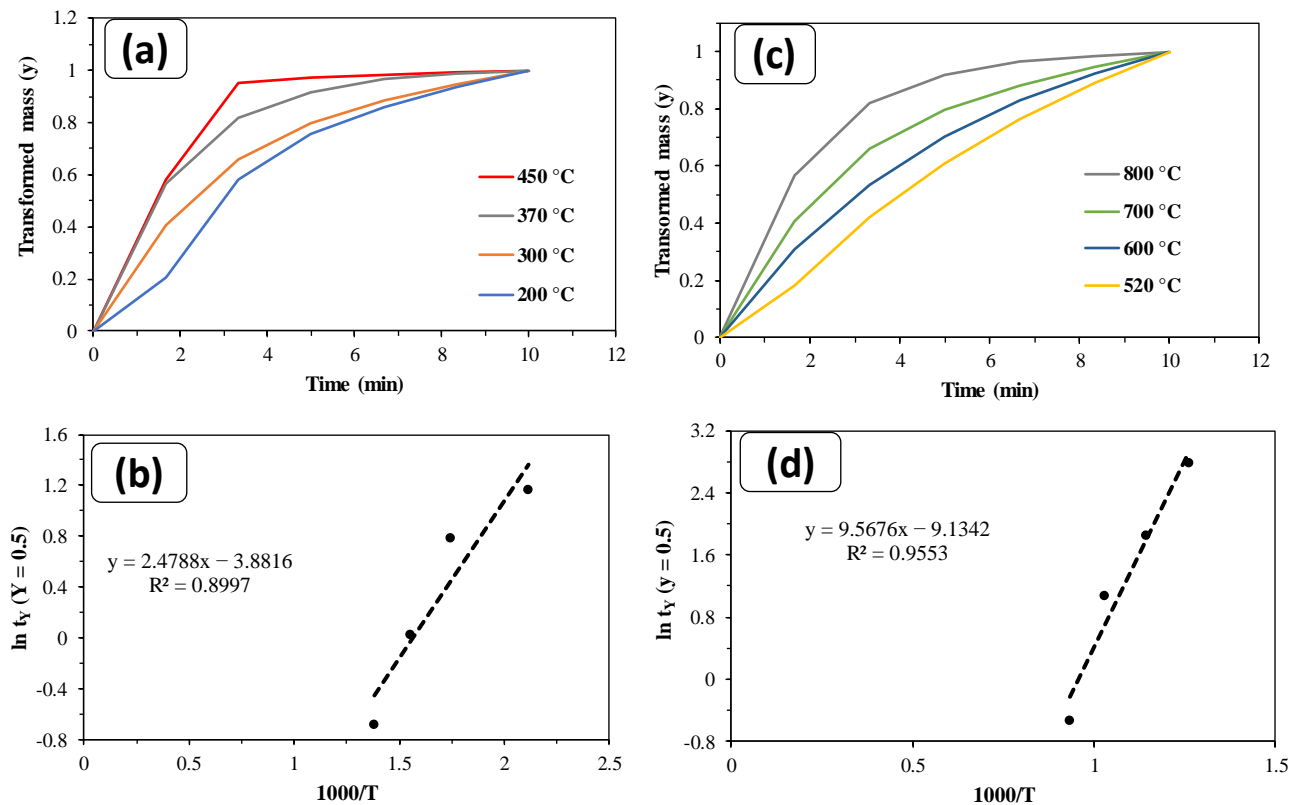


Figure 7. Kinetic analysis of thermal decomposition of carbon nanotubes decorated with magnetite nanoparticles. (a) First-stage mass loss isotherms of carbon nanotubes decorated with magnetite nanoparticles; (b) calculation of the first-stage activation energy of carbon nanotubes decorated with magnetite nanoparticles; (c) second-stage mass loss isotherms of carbon nanotubes decorated with magnetite nanoparticles; (d) calculation of the second-stage activation energy of carbon nanotubes decorated with magnetite nanoparticles.

4. Conclusions

Multiwalled carbon nanotubes with diameters ranging from 10 to 30 nm and varying lengths were synthesized and decorated with magnetite nanoparticles with diameters ranging from 15 nm to 35 nm and spherical morphology. X-ray diffraction showed that the nanotubes are made of carbon and magnetite of nanometric sizes. The decoration of the carbon nanotubes was carried out and verified by scanning electron microscopy, where it was observed that they were superficially decorated. Thermal decomposition shows that there are two mass losses for both the decorated nanotubes and those analyzed without decoration; the activation energy of the first mass loss of the undecorated nanotubes is 6.75 kJ/mol, and the second loss is 25.74 kJ/mol, which indicates that the transport of matter controls these mass losses. The thermal decomposition of the decorated carbon nanotubes also shows two mass losses, of which the first mass loss has an activation energy of 20.61 kJ/mol, which indicates a mixed control, but this is mostly controlled by the transport of matter; however, for the second mass loss, this has an activation energy of 79.54 kJ/mol, which indicates that the thermal decomposition of the second stage is controlled by the chemical reaction, which indicates that the temperature is completely what controls this last process. The decorated carbon nanotubes present greater thermal stability; this is because the decoration works as a shell that makes them withstand higher decomposition temperatures and that high energies are required for said decomposition to take place.

Author Contributions: Formal analysis, R.H.O. and E.G.P.; investigation, I.A.R., M.U.F. and L.G.-H.; methodology, J.-C.G.-I., J.C.J. and M.R.; supervision, S.O. and P.A.R.-O. All authors have read and agreed to the published version of the manuscript.

Funding: This research received no external funding.

Data Availability Statement: All data presented are original.

Acknowledgments: Praise the Lord Jah for Your Eternal Glory.

Conflicts of Interest: The authors declare no conflicts of interest.

References

1. Hawryla, M.; Fernandes Macedo, M.L.; Rocco, A.M. Technology of carbon nanotubes: Trends and perspectives of multidisciplinary area. *Divulg. Quím. Nova*. **2024**, *27*, 986–992. [[CrossRef](#)]
2. Ali, Z.; Yaqoob, S.; D'Amore, A. Impact of Dispersion Methods on Mechanical Properties of Carbon Nanotube (CNT)/Iron Oxide (Fe₃O₄)/Epoxy Composites. *C* **2024**, *10*, 66. [[CrossRef](#)]
3. Bala, K.; Sharma, D.; Gupta, N. Carbon-Nanotube–Based Materials for Electrochemical Sensing of the Neurotransmitter Dopamine. *Chem. Electro. Chem.* **2019**, *6*, 274–288. [[CrossRef](#)]
4. Kumar, S.; Sharma, R.; Singh, D.; Awasthi, A.; Kumar, V.; Singh, K. Tungsten sulphide decorated carbon nanotube based electroanalytical sensing of neurotransmitter dopamine. *Electrochim. Acta* **2024**, *475*, 143584. [[CrossRef](#)]
5. Zhao, J.; Xie, R.H. Electronic and photonic properties of doped carbon nanotubes. *J. Name J. Nanosci. Nanotechnol.* **2003**, *3*, 459–478. [[CrossRef](#)]
6. Zhang, Y.; Xu, Y.; Liu, H.; Sun, B. Ultrahigh sensitivity nitrogen–doping carbon nanotubes-based metamateria–free flexible terahertz sensing platform for insecticides detection. *Food Chem.* **2022**, *394*, 133467. [[CrossRef](#)]
7. Katta, S.S.; Yadav, S.; Singh, A.P.; SanthiBhushan, B.; Srivastava, A. Investigation of pristine and B/N/Pt/au/Pd doped single-walled carbon nanotube as phosgene gas sensor: A first-principles analysis. *Appl. Surf. Sci.* **2022**, *588*, 152989. [[CrossRef](#)]
8. Song, Y.; Zhang, T.; Zhou, G.; Liu, P.; Yan, X.; Xu, B.; Guo, J. Cu nanoclusters on N-doped carbon nanotubes as efficient electrocatalyst for oxygen reduction reaction. *Appl. Surf. Sci.* **2022**, *589*, 153022. [[CrossRef](#)]
9. Kakil, S.A.; Abdullah, H.Y. Pt– and Pd-doped carbon nanotubes with different diameters as CO sensors: A comparative DFT study. *Diam. Relat. Mater.* **2023**, *139*, 110311. [[CrossRef](#)]
10. Yoosefian, M.; Etminan, N. Density functional theory (DFT) study of a new novel bionanosensor hybrid; tryptophan/Pd doped single walled carbon nanotube. *Phys. E Low–Dimens. Syst. Nanostruct.* **2016**, *81*, 116–121. [[CrossRef](#)]
11. Deng, S.; Jian, G.; Lei, J.; Hu, Z.; Ju, H. A glucose biosensor based on direct electrochemistry of glucose oxidase immobilized on nitrogen-doped carbon nanotubes. *Biosens. Bioelectron.* **2009**, *25*, 373–377. [[CrossRef](#)] [[PubMed](#)]
12. Zhao, L.; Chai, M.H.; Yao, H.F.; Huang, Y.P.; Liu, Z.S. Molecularly imprinted polymers doped with carbon nanotube with aid of metal–organic gel for drug delivery systems. *Pharm. Res.* **2020**, *37*, 193. [[CrossRef](#)] [[PubMed](#)]
13. Ang, L.M.; Hor, T.S.A.; Xu, G.Q.; Tung, C.H.; Zhao, S.P.; Wang, J.L.S. Decoration of activated carbon nanotubes with copper and nickel. *Carbon* **2000**, *38*, 363–372. [[CrossRef](#)]
14. Wang, J.; Mi, Z.; Lu, C.; Han, Z.; Wu, Y.; Fu, X.; Zhang, G. Preparation of carbon nanotube-filled bismuth/tin green nanocomposites and their efficient catalytic activity in the thermal decomposition of ammonium perchlorate. *Surf. Interfaces* **2024**, *45*, 103866. [[CrossRef](#)]
15. Gao, J.M.; Wang, L.; Yu, H.J.; Xiao, A.G.; Ding, W.B. Recent research progress in burning rate catalysts. *Propellants Explos. Pyrotech.* **2011**, *36*, 404–409. [[CrossRef](#)]
16. Xu, R.Z.; Yang, L.F.; Fang, H.C.; Mi, Z.Y.; Lv, Y.P.; Jiang, L.P.; Fu, X.L.; Li, J.Z.; Zhang, G.F. Copper complexes in carbon nanotubes as catalysts for thermal decomposition of energetic oxidizers. *ACS Appl. Nano Mater.* **2022**, *5*, 14942–14953. [[CrossRef](#)]
17. Yang, L.F.; Xu, R.Z.; Mi, Z.Y.; Wan, Y.T.; Fu, X.L.; Jiang, L.P.; Jian, Y.J.; Li, J.Z.; Zhang, G.F. Enhanced anti-migration performance of carbon nanotubes confined ferrocenyl compounds and their synergistic catalytic activity on the thermal decomposition of ammonium perchlorate. *Mater. Today Chem.* **2022**, *26*, 101168. [[CrossRef](#)]
18. Yang, L.F.; Mi, Z.Y.; Fang, H.C.; Xu, R.Z.; Lv, B.Y.; Li, J.Z.; Zhang, G.F. Fabrication of highly catalytic active α -Fe₂O₃–carbon nanotube composites for thermal decomposition of ammonium perchlorate by light and temperature control strategy. *Surf. Interfaces* **2024**, *44*, 103642. [[CrossRef](#)]
19. Fang, H.C.; Xu, R.Z.; Yang, L.F.; Mi, Z.Y.; He, Q.; Shi, H.F.; Jiang, L.P.; Fu, X.L.; Zhang, G.F. Facile fabrication of carbon nanotubes–encapsulated cobalt (nickel) salt nanocomposites and their highly efficient catalysis in the thermal degradation of ammonium perchlorate and hexogen. *J. Alloys Compd.* **2022**, *928*, 167134. [[CrossRef](#)]
20. Xu, X.; Hu, J.Q.; Yang, S.Z.; Xie, F.; Guo, L. Extreme pressure synergistic mechanism of bismuth naphthenate and sulfurized isobutene additives. *Surf. Rev. Lett.* **2017**, *24*, 1750071. [[CrossRef](#)]
21. Altaf, S.; Zafar, R.; Zaman, W.Q.; Ahmad, S.; Yaqoob, K.; Syed, A.; Khan, A.J.; Bilal, M.; Arshad, M. Removal of levofloxacin from aqueous solution by green synthesized magnetite (Fe₃O₄) nanoparticles using *Moringa olifera*: Kinetics and reaction mechanism analysis. *Ecotoxicol. Environ. Safe.* **2021**, *226*, 112826. [[CrossRef](#)] [[PubMed](#)]
22. Diaz, E.; Mejía, C.; Ortiz, J. Microsture analysis of multiwall carbon nanotubes purified by oxidation and ionic and covalent functionalization. In Proceedings of the International Conference On Diamont and Carbon Materials, Madrid, Spain, 7–11 September 2014; 2014.

23. Hamouda, H.I.; Abdel–Ghafar, H.M.; Mahmoud, M.H.H. Multi–walled carbon nanotubes decorated with silver nanoparticles for antimicrobial applications. *J. Environ. Chem. Eng.* **2021**, *9*, 105034. [[CrossRef](#)]
24. Putnis, A. *Introduction to Mineral Sciences*, 3rd ed.; Cambridge University Press: Cambridge, UK, 1992; pp. 154–196.
25. Ballester, A.; Verdeja, F.; Sancho, J. *Metalurgia Extractiva*, 2nd ed.; Síntesis: Barcelona, Spain, 2000; pp. 154–196.
26. Levenspiel, O. *Ingeniería de las Reacciones Químicas*, 2nd ed.; Reverté: Barcelona, Spain, 2002.
27. Torrente, M.C.; Galán, M.A. Kinetics of the thermal decomposition of oil shale from Puertollano (Spain). *Fuel* **2001**, *80*, 327–334. [[CrossRef](#)]
28. Majumdar, S.; Sharma, I.G.; Bidaye, A.C.; Suri, A.K. A study on isothermal kinetics of thermal decomposition of cobalt oxalate to cobalt. *Thermochim. Acta* **2008**, *473*, 45–49. [[CrossRef](#)]

Disclaimer/Publisher’s Note: The statements, opinions and data contained in all publications are solely those of the individual author(s) and contributor(s) and not of MDPI and/or the editor(s). MDPI and/or the editor(s) disclaim responsibility for any injury to people or property resulting from any ideas, methods, instructions or products referred to in the content.